ACCEPTED FOR PUBLICATION IN APJ
Preprint typeset using LaTeX style emulateapj v. 11/26/04

RESONANCE OVERLAP IS RESPONSIBLE FOR EJECTING PLANETS IN BINARY SYSTEMS

LAWRENCE R. MUDRYK AND YANQIN WU
Department of Astronomy and Astrophysics, University of Toronto, Toronto, ON M5S 3H8

ABSTRACT

A planet orbiting around a star in a binary system can be ejected if it lies too far from its host star. We find that instability boundaries first obtained in numerical studies can be explained by overlap between sub-resonances within mean-motion resonances (mostly of the j:1 type). Strong secular forcing from the companion displaces the centroids of different sub-resonances, producing large regions of resonance overlap. Planets lying within these overlapping regions experience chaotic diffusion, which in most cases leads to their eventual ejection. The overlap region extends to shorter-period orbits as either the companion's mass or its eccentricity increase. Our analytical calculations reproduce the instability boundaries observed in numerical studies and yield the following two additional results. Firstly, the instability boundary as a function of eccentricity is jagged; thus, the widest stable orbit could be reduced from previously quoted values by as much as 20%. Secondly, very high order resonances (e.g., 50:3) do not significantly modify the instability boundary despite the fact that these weak resonances can produce slow chaotic diffusion which may be missed by finite-duration numerical integrations. We present some numerical evidence for the first result. More extensive experiments are called for to confirm these conclusions. For the special case of circular binaries, we find that the Hill criterion (based on the critical Jacobi integral) yields an instability boundary that is very similar to that obtained by resonance overlap arguments, making the former both a necessary and a sufficient condition for planet instability.

Subject headings: binaries:general—gravitation—instabilities—planetary systems

1. INTRODUCTION

The majority of solar-type stars in our neighborhood ($\sim$ 60%) are in binary or higher-multiple systems (Duquennoy & Mayor 1991). Despite this majority, there are still questions as to how many of these multiple-star systems host planets, and whether or not the planet formation process inside these systems differs markedly from that around single stars. Radial-velocity surveys have shown that $\sim$ 20% of the extra-solar planets reside in binaries (Eggenberger et al. 2004), but the true fraction is likely higher as these surveys select against observing known binaries.

While it is clear that much theoretical and observational effort is still needed to fully answer the above questions, much progress has been made in one sub-area of this issue—the dynamical stability of planets in binary systems. The body of literature on this topic is extensive, with most studies using numerical techniques. Hénon & Guyot (1970) numerically studied periodic planet orbits in circular binaries (circular restricted problem) as a function of the binary mass ratio. Benest (1993) included binary eccentricity in his study but only focused on a few astronomical systems. Rabl & Dvorak (1988) also considered eccentric binaries but limited their studies to equal-mass stars. Holman & Wiegert (1999, hereafter HW99) is the most comprehensive and homogeneous study to date. They numerically integrated (initially circular) planet orbits for 10^4 binary periods, and charted out the stability region as a function of binary separation, eccentricity, and mass ratio, for both the S-type (circum-stellar) and P-type (circum-binary) planetary orbits. Pilat-Lohinger & Dvorak (2002) have since included the effect of planet eccentricity but found it to be less important than the binary eccentricity. With the intention to quantify the confines of habitable zones around binary stars, Musielak et al. (2005) also investigated the stability of both S-type and P-type planetary orbits in circular binaries. To this end, they adopted a criterion for stability that differs slightly from that used in other works. However, they found results that largely agree with those from previous works, including those of HW99. Marzari et al. (2005) examined the stability of multiple planets in binary systems, including the effects of mutual planetary perturbations. In this case, interactions among the planets themselves appear to be the leading cause for instability. David et al. (2003) concentrated on studying ejection timescales for planets within the unstable region. They established an empirical formula for the ejection timescale that is a steep function of the periastron distance for the binary companion. Beyond a certain distance, however, this trend is expected to break down and the ejection time become infinite (the system becomes stable). The location of this break is the boundary for which we are interested in searching. Since the afore-mentioned papers have confirmed the HW99 results, we focus on comparing our analytical results against those of HW99 exclusively.

The numerical results of HW99 and Rabl & Dvorak (1988) uphold the expectation that the stability space (comprising the binary's eccentricity and the ratio of the planet's semi-major axis to that of the binary) shrinks with decreasing stellar separation, with increasing orbital eccentricity, and with increasing companion mass. However, the underlying physical mechanism for planet ejection has yet to be demonstrated. Moreover, current computational capabilities limit the integration time (up to 10^4 binary orbits in HW99) and permit only coarse-grid parameter searches. The former limitation may allow longer-term instabilities to be missed while the latter blurs the transition from stability to instability, hiding the existence of possible '(in-)stability islands.'

Our current study aims to overcome these limitations. We expose the instability mechanism, delineate the topology of transition between stability and instability, and exclude the possible existence of longer-term instabilities. We accomplish these aims by studying individual orbital resonances and the conditions for which they overlap, adopting resonance overlap as a necessary and sufficient criterion for chaotic diffu-

Electronic address: mudryk@astro.utoronto.ca

sion, and consequentially, for planet instability. In this work, we focus our attention on the orbits most relevant for radial-velocity searches—the so-called S-type orbits (Dvorak 1984), where the planet orbits around one of the stars. The second star is considered to be an external perturber. We also limit our studies, like most numerical works, to coplanar systems. Non-coplanarity introduces new resonances, which may render the systems more unstable.

In this paper, we first present analytical arguments that allow us to determine the boundaries of stability (§2) and then compare them against numerical results from HW99 (§3). We dedicate a special section to the case of circular restricted problem (§4) and present our conclusions in §5.

2. RESONANCE OVERLAP

Chaotic diffusion associated with resonance overlap has been shown to be responsible for all known cases of instability in the solar system, including the clearing of the Kirkwood gaps within the asteroid belt and the orbital stability of planets and short-period comets (Wisdom 1980a; Dermott & Murray 1983). In this context, the most massive perturber, Jupiter, has a mass ratio to the Sun of $\sim 10^{-3}$, and in addition to (fairly low-order) 2-body mean-motion resonances, both secular resonances and 3-body resonances have also been shown to be relevant (for a review, see Lecar et al. 2001).

The situation in a binary system is different. The companion star is the lone perturber with a mass ratio of order unity. The only relevant resonances are the 2-body mean-motion resonances (MMRs), but these are not limited only to low-order.

Despite having $\mu = m'/(m_c+m') \sim 1$ in our case, where m' is the companion mass and m_c the host star mass, we adopt the formalism of the disturbing function formally derived for $\mu \ll 1$. We believe that this formalism includes all relevant resonant angles and correctly describes the resonance strength to order unity, which is sufficient for our purpose (more later). The disturbing function for the planetary orbit has the form (Murray & Dermott 1999, hereafter MD99)

$$\mathcal{R} = \frac{Gm'}{a'} \sum S_j \cos\varphi_j, \tag{1}$$

where a' is the semi-major axis of the binary companion. We use primed variables for the orbital elements of the binary companion, and unprimed variables for those of the planet (which has mass m). S_j is a coefficient that depends on the eccentricities of the planet and the external companion, and on the ratio of their semi-major axes, $\alpha = a/a'$. The mean motion, n, is expressed as $n^2 = G(m_c+m)/a^3$. The angle argument is

$$\varphi_j = j_1\lambda' + j_2\lambda + j_3\varpi' + j_4\varpi, \tag{2}$$

where ϖ is the longitude of pericentre, and λ is the mean longitude. The mean longitude and mean motion are related by $\lambda = nt+\epsilon$ where ϵ is the mean longitude at epoch. Similar relations exist for the companion. The summation in equation (1) is formally over all integer combinations (j_1, j_2, j_3, j_4) that satisfy the *d'Alembert relation*: $j_1+j_2+j_3+j_4 = 0$. However, at a given α value, only a few combinations are relevant for the dynamics—for the other combinations, the angle φ_j varies with time too fast to have any sustained long-term effect. Removing these fast oscillating terms by integrating over an appropriately long time and keeping terms to the lowest order in eccentricities, we obtain the averaged disturbing function,

$$\mathcal{R} = \frac{Gm'}{a'}\left[f_{s1}(e^2+e'^2) + f_{s2}ee'\cos(\varpi'-\varpi) + f_r e'^{|j_3|}e^{|j_4|}\cos\varphi_j\right]. \tag{3}$$

The first two terms in the brackets arise from the two lowest order secular interactions, while the last term accounts for MMRs situated at $j_1n' + j_2n \approx 0$. In particular, these could include resonances that share the same j_1 and j_2 values but have different j_3 (and therefore j_4) values. We call these 'subresonances' of a given MMR (j_1, j_2). Their importance will become clear later. The coefficients f_{s1} and f_{s2} are functions of α alone. Explicit expressions for them are presented in Table B.3 of MD99. The f_r coefficient depends on α as well as the particular resonance under consideration. MD99 cited two expansion formulas (eqs. [6.36] and [6.113] in MD99) to calculate the interaction strength for any resonance and listed explicit expressions for low-order resonances (Appendix B of MD99). We find that both expansion formulas yield similar results and agree with the explicit formula at low-order. These expansions diverge for $e' > 0.6627434$ (see MD99), so we limit our studies to $e' < 0.6$.

Variations of the planet's orbital elements are obtained using Lagrange's equations as

$$\dot{n} = 3j_2C_rne'^{|j_3|}e^{|j_4|}\sin\varphi_j, \tag{4}$$

$$\dot{e} = -C_{s2}e'\sin(\Delta\varpi) + j_4C_re'^{|j_3|}e^{|j_4|-1}\sin\varphi_j, \tag{5}$$

$$\dot{\varpi} = 2C_{s1} + C_{s2}\frac{e'}{e}\cos(\Delta\varpi) + |j_4|C_re'^{|j_3|}e^{|j_4|-2}\cos\varphi_j, \tag{6}$$

$$\dot{\epsilon} = C_{s1}e^2 + \frac{C_{s2}}{2}e'e\cos(\Delta\varpi) + \frac{|j_4|}{2}C_re'^{|j_3|}e^{|j_4|}\cos\varphi_j, \tag{7}$$

where $\Delta\varpi$ is the secular angle argument, $\Delta\varpi = \varpi'-\varpi$. Moreover, the C-coefficients are related to the f-coefficients in equation (3) by $C_x = [Gm'/(na^2a')]f_x \approx (m'/m_c)n\alpha f_x(\alpha)$. The variation in ϵ is smaller than that in ϖ by a factor of e^2 and can be neglected. Perturbations of the companion's orbital elements due to the planet are also ignored.

Exact resonance occurs when both $\sin\varphi_j = 0$ and $\dot{\varphi}_j = 0$, *viz.* $j_1n' + j_2n + j_4\dot{\varpi} = 0$. Near this location, φ_j librates about the resonant value. Moving away from this location, there exists a boundary beyond which φ_j changes from libration to circulation. This boundary defines the *width* of the resonance, namely, the range of space over which the resonance dominates the planet's dynamics. When the widths of two resonances become comparable to their separation, the planet can be affected simultaneously by these overlapping resonances. Mathematically, the overlap of two or more resonances causes neighboring trajectories to diverge exponentially with time (Chirikov 1979; Wisdom 1980a). This occurs on the Lyapunov timescale (T_L), which, as argued by Holman & Murray (1996), is comparable to the libration timescale for the resonances in question. Except in the case of 'bounded chaos,' orbital parameters for the planet undergo unbounded random walks leading to ejection on a timescale called the event timescale (T_e). Though T_e fluctuates depending on the system, studies have shown that it roughly correlates with T_L (see, e.g. Lecar et al. 1992).

In our problem, the large companion mass produces strong secular forcing, making it different from typical solar-system dynamics problems. Firstly, even if the planet initially has zero eccentricity, it is forced to oscillate with an eccentricity amplitude (eqs. [5] and [6])

$$e_{\rm sec} = \frac{C_{s2}}{2C_{s1}}e', \tag{8}$$

on the short secular timescale $\Delta t \sim 2\pi/(2C_{s1})$. The magnitude of $e_{\rm sec}$ decreases with decreasing α but can be as large

as $e'/2$ near the 3:1 resonance. We find that $e_{\rm sec} \sim \alpha e'$. For equal-mass binaries, the secular timescale ranges from ~ 20 planet orbital periods at the 3:1 resonance to ~ 1000 periods at the 20:1 resonance. While the secular timescale is likely too long when compared with the mean-motion of the companion to allow for the 'evection resonance' (Touma & Wisdom 1998),[1] it is typically much shorter than the resonant timescale. Considering also that the resonant strength is at maximum when the value of e is at its largest, we can assume that $e = e_{\rm sec}$ for the resonant interactions. Planets possessing a free eccentricity in addition to the forced value can reach higher overall eccentricity and will therefore be more unstable.

The second effect of the companion's strong secular forcing is to displace the centroid of different sub-resonances away from each other. In Appendix A, we derive expressions for the centroid and the width of a resonance when secular forcing is important. While the width remains unchanged from the non-secular case, the centroid of a MMR is shifted from its nominal position, ($j_1 n' + j_2 n = 0$), by an amount, $|\delta n| \sim |2(j_4/j_2)C_{s1}|$. As a result, the region of resonance overlap is greatly expanded. This effect is illustrated in Fig. 1 for two groups of MMRs.

Resonance overlap generates chaotic diffusion, but as pointed out by Murray (1992), under some circumstances resonance overlap will lead only to 'bounded chaos'—unpredictable but limited variations in the orbital elements. One such example is provided by Gladman (1993). Results from our numerical experiments (Fig. 2) as well as discussions in §4 suggest that this is not a major concern for determining the instability boundary. In the remaining discussion we, therefore, do not distinguish between the concepts of resonance overlap and planet instability.

Another question relates to whether the overlap between sub-resonances is as potent as that between distinct MMRs, thereby leading to planet instability on an astronomically interesting timescale (see the review by Malhotra 1998). We present calculations in §3 which suggest that this is indeed so.

3. COMPARISON WITH HW99 AND DISCUSSION

In our determination of regions of resonance overlap, we include resonances with $j_1 \geq 3$, $-4 \leq j_2 \leq -1$, and $-|j_1 + j_2| \leq j_3 \leq 0$. We restrict the value of j_2 since the strength of a resonance scales as $e'^{|j_3|} e^{|j_4|} \propto e'^{|j_1+j_2|}$ (eq. [3]). For a given orbital separation, α, the ratio of j_2/j_1 is determined by Kepler's third law: $\alpha^3 = (j_2/j_1)^2(1-\mu)$; hence, the strongest resonances have $j_2 = -1$. In fact, we show that even the $j_2 = -4, -3$, and -2 resonances do not affect the instability boundary much. Moreover, while $j_3 = 0$ is the strongest sub-resonance in solar system dynamics (in light of Jupiter's small eccentricity), we find here that all sub-resonances are essential to determine the overlap region.

Coupling strengths are calculated using the aforementioned series expansion formulas in MD99 (eqs. [6.36] or [6.113]). The location and width of each resonance are obtained as described in Appendix A. Planet eccentricity is taken to be the secularly-forced value (eq. [8]). All coefficients are evaluated at exact resonance, assuming the resonance width is small. In the (α, e') phase space, a region is designated as unstable if more than one resonance (or sub-resonance) spans it. We further assign a similar status, at the same value of e', to the entire extent in α of the sub-resonance in which this region is situated (see Fig. 1). Depending on its orbital phase, a planet situated within a single resonance (elsewhere spanned by additional resonances), but which is still outside of the region of overlap proper, may (or may not) librate into the latter. This definition of unstable regions ensures that all potentially unstable orbits are included. Again, our analytical study is limited to $e' < 0.6$ to ensure a converging disturbing function.

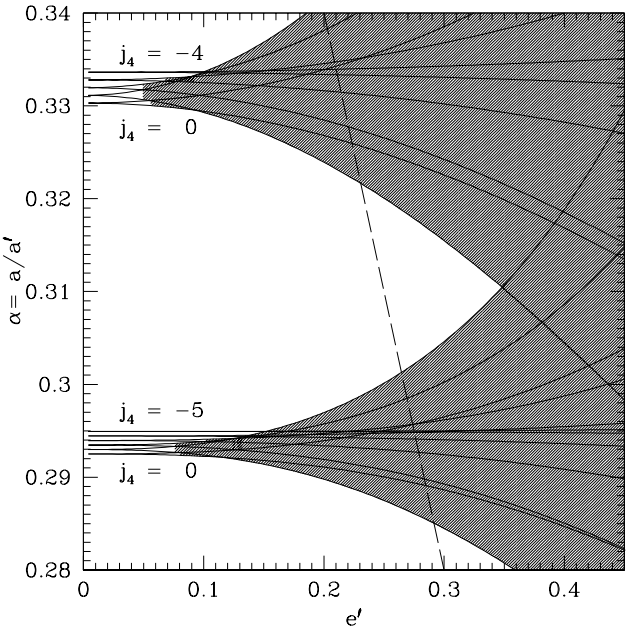

FIG. 1.—Location and width of various sub-resonances as a function of e', obtained for a $\mu = 0.1$ binary. The top group are the sub-resonances of the 5:1 MMR (identified by their respective j_4 values) and the lower group, of the 6:1 MMR. We take the planet eccentricity to be the secularly-forced value. The centroids of different sub-resonances within a distinct MMR are displaced from each other due to both secular and resonant forcing though the secular effect dominates at low values of e'. Shaded regions are regions of instability, as defined in the text. Overlap between sub-resonances of the same MMR covers a much larger region than overlap between distinct MMRs.

Our full results are shown in Fig. 2 for mass-ratio $\mu = 0.1$, and in Fig. 3 for $\mu = 0.5$. As has been indicated in Fig. 1, the instability boundary is jagged, with jutting peninsulas and narrow inlets. This is different from the smooth lines presented by HW99. However, their curves largely trace the outline of our results. The two sets of results can be considered consistent since HW99 carried out their investigation over a crude grid in $\alpha - e'$ space. To confirm this, we perform similar numerical integrations, with a much finer grid in a selected region of $\alpha - e'$ space. We adopt the Hierarchical Jacobi Symplectic integrator by Beust (2003), an add-on to the SWIFT package (Duncan et al. 1998) for studying dynamics in multiple-star stellar systems. Planets are initialized to have random orbital phases and an eccentricity given by $e = e_{\rm sec}$ (initializing planets with zero eccentricity produces similar results). We integrate their orbits for 3000 binary periods. The stability of these orbits is indicated in the inset of Fig. 2. The detailed topology agrees well with that obtained from our perturbation analysis, and in many cases, one can even identify the (sub)-resonances responsible for the instability. This suggests that resonance overlap and the consequential chaotic diffusion is the mechanism responsible for the planet instability observed in HW99's numerical investigation. Moreover,

[1] When the companion mass dominates, $\mu \to 1$, the evection resonance may become important. See §4.

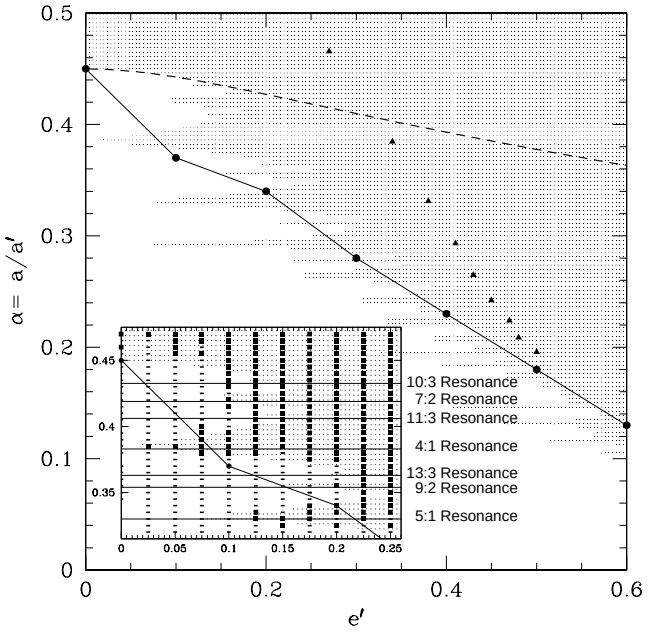

FIG. 2.—Stability diagram for planets in a $\mu = 0.1$ binary system. The solid curve connecting filled circles locates the maximum stable value of $\alpha = a/d$ as obtained by HW99 while dots map regions of instability caused by resonance overlap. Resonances included in this calculation are described in the text. The instability boundary as it exists when considering only the distinct MMRs (keeping $j_3 = 0$) is denoted by filled triangles. Over the eccentricity range of interest, overlap between sub-resonances is the most significant source of planet instability. As $e' \to 0$, widths of most resonances approach 0 except for the 2:1 and 3:1 resonances. The dashed curve shows the lower confine of a 3:1 resonance—overlap between sub-resonances within the 3:1 MMR can explain instability in circular binaries. **Inset:** results of numerical integration over a selected region of $\alpha - e'$ space. Dashes represent planet orbits that remain stable for more than 3000 binary periods; filled squares represent unstable orbits. Horizontal lines indicate centroid locations of certain MMRs that are responsible for the jutting peninsulas. At each e' value, $j_2 = -1$ MMRs yield the shortest-period unstable orbits. Stability for points near the instability boundary are sensitive to the initial conditions. Regions of resonance overlap coincide with that for planet instability and there is little evidence for 'bounded chaos.'

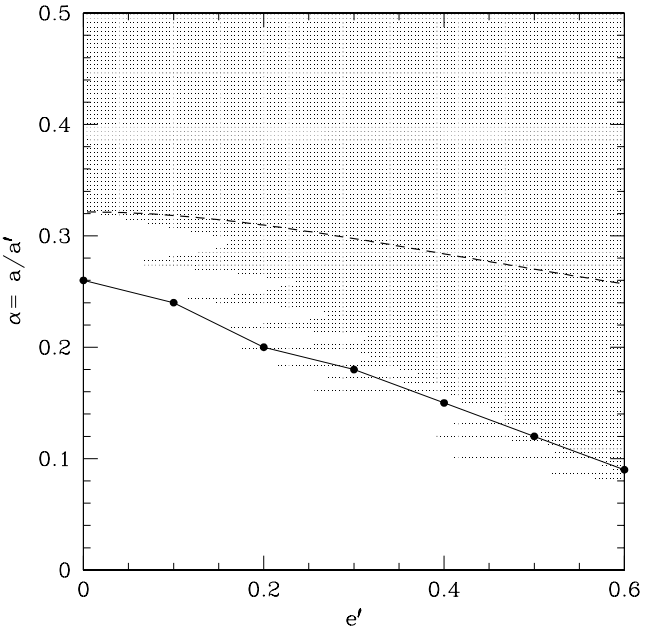

FIG. 3.—Stability diagram for planets in an equal-mass binary system ($\mu = 0.5$). Symbols are the same as those in Fig. 2. We obtain these results using a perturbation formula that is strictly valid only for $\mu \ll 1$—this may account for some of the discrepancy between our results (dots) and those of HW99 (solid curve).

there is little evidence for 'bounded chaos' near the instability boundary, so that one can adopt the boundary of resonance overlap as the boundary for planet instability.

In an effort to delineate the differences between the chaotic dynamics existing within regions of resonance overlap and the regular dynamics existing just outside such regions, we numerically integrate two sets of two initially 'close' planets. Both sets of planets are situated near the 5:1 MMR in a binary system with mass ratio, $\mu = 0.1$, and eccentricity, $e' = 0.2$. The first set of two planets are situated directly within the region of overlap at $\alpha = 0.33$, while the second set are situated just outside the region of overlap at $\alpha = 0.32$. Fig. 4 presents the results of integrating the first set of two planets initialized with identical orbital parameters except for a tenth of a degree difference in their orbital phase positions. The Lyapunov timescale is defined as the timescale for exponential divergence between two infinitesimally close orbits. We roughly estimate this timescale for the trajectories presented in Fig. 4 and obtain $T_L \approx 10$ binary orbits. De-correlation in the semi-major axis and eccentricity becomes apparent to the eye after approximately 50 binary orbits. The libration time within this resonance, which one expects to be of the same order as the Lyapunov time, is ~ 54 binary orbits. The planets are ejected in turn after about 1500 and 3800 binary orbits. Further integrations at the same location with different initial orbital phases show a wide spread in the ejection times ranging from 50–4000 binary orbits, corresponding to $\sim 10^4 - 10^6$ years for a solar-mass binary at 50 AU. Murray & Holman (1997) and David et al. (2003) presented two different empirical expressions that relate the (widely scattered) ejection time (T_e) to the Lyapunov timescale. The former found a relationship between these two timescales (applicable to overlapping sub-resonances) given by $T_e/T' = 10^a (T_L/T')^b$ where $a = 1.45$ and $b = 1.68$, and where T' denotes the binary orbital period. Applying this formula to our case yields an ejection time of $T_e/T' \sim 2000$. The expression by David et al. (2003) yields a comparable value of $T_e/T' \sim 7400$. Within the scatter, both values agree with our experiments.

Adopting the expression by Murray & Holman (1997), we obtain ejection times for various resonances. Lower order resonances lead to faster ejection, while at the higher end, for example, the 30:1 resonance, we find $T_e/T' \leq 10^6$ for a system with mass-ratio, $\mu = 0.1$. This resonance (corresponding to $\alpha = 0.10$) defines the maximum stable orbit for the most eccentric binary orbit we consider ($e' = 0.66$). The ejection time corresponds to ~ 400 Myrs for a 50 AU binary and ~ 1 Gyrs for a 100 AU binary (all assuming a total system mass equal to one solar-mass). We conclude that overlap of sub-resonances leads to planet ejection on astronomically interesting timescales, for the parameters we have considered.

By contrast, the results of the second set of integrations where we instead situate the two planets just outside the region of resonance overlap at a location given by $\alpha = 0.32$, do not exhibit sensitivity on the initial conditions and no planet is ejected within our integration time ($10^4 T'$). The transition to instability occurs over a narrow region.

One major discrepancy between our results and those of

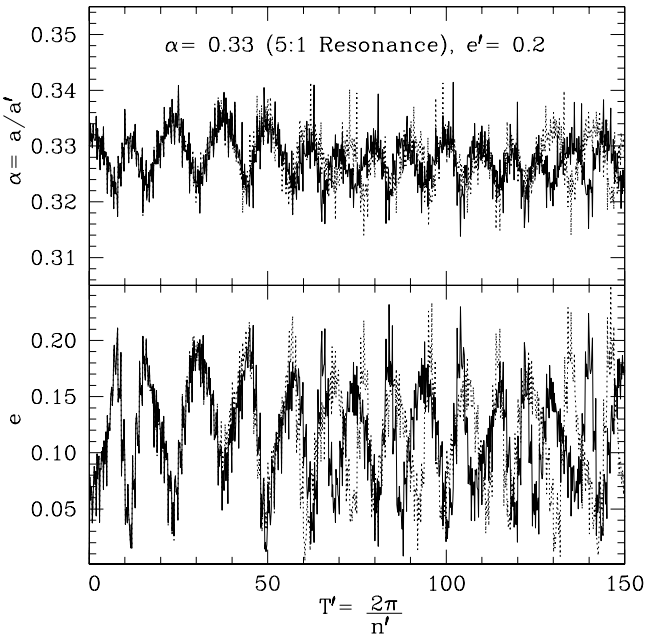

FIG. 4.—Numerical integration of two planets initialized with identical orbital parameters except for a tenth of a percent difference in the initial orbital phase. The resulting semi-major axis and eccentricity are plotted as functions of time (measured in binary orbital periods, T') in solid (or dotted) curves for each planet. The Lyapunov timescale is estimated to be ~ 10 binary orbits, and de-correlation in the semi-major axis and eccentricity becomes apparent to the eye after approximately 50 binary orbits. The planets are ejected in turn after about 1500 and 3800 orbits.

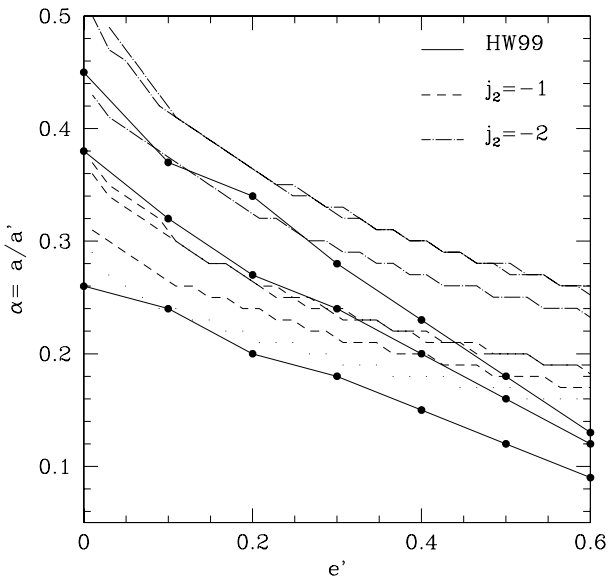

FIG. 5.—Comparison of instability boundaries obtained based on simple approximations of our analytical arguments (eq. [10]) and numerical results of HW99. The group of dashed curves represent the approximate overlap condition for $j_2 = -1$ MMRs, while the dot-dashed ones represent those for $j_2 = -2$ MMRs, both with $|j_4| = j_1/2$. Within each group, from top to bottom, the value of the mass-ratio is $\mu = 0.1, 0.2$ (these two curves almost coincide), and 0.5, respectively. If we recalculate the bottom-most dashed curve ($\mu = 0.5$) assuming the value of C_{s1}/C_r is 10 times smaller, we obtain the results shown in the dotted curve.

HW99 can be observed in Fig. 3 for equal-mass binaries: at low binary eccentricity, the HW99 curve falls below that obtained from our perturbation analysis. This likely reflects failure of the expansion formula when μ is large (more below).

A key question of interest asks, what is the longest-period stable planet orbit, for a given binary (fixed μ and e')? HW99 provided a fitting formula for the minimum unstable α as a function of μ and e'. Our results here indicate, however, that the minimum unstable α should be reduced by up to $\sim 20\%$ from their values. This is related to the thin instability peninsulas evident in our Figs. 2 and 3.

In order to understand how the outline of the instability boundary depends on various parameters, we propose the following rough scaling argument. Let neighboring sub-resonances be spaced by Δn, where due to secular forcing, $\Delta n \approx 2|C_{s1}/j_2|$ (eq. [A5]). Resonant interactions also modify the centroid of a resonance, but they are less important than the secular effect for small e'. The width of an individual sub-resonance, k, is expressed in equation (A6), which in most cases can be simplified as $k \approx [4j_4^2/(3j_2)]|C_r|e'^{|j_3|}e^{|j_4|-2}$. Adopting $e = e_{\rm sec} \approx \alpha e'$, and requiring resonance overlap ($\Delta n < 2k$), we find that instability occurs when

$$\alpha \geq \alpha_{\rm crit} = \left(\frac{3}{4|j_4|^2 e'^{|j_1+j_2|-2}} \left| \frac{C_{s1}}{C_r} \right| \right)^{1/(|j_4|-2)} . \qquad (9)$$

Defining $f_4 = |j_4/j_1|$, and relating j_1 to α by Kepler's Law, $|j_1/j_2|^2\alpha^3 = 1-\mu$, we recast equation (9) as

$$\alpha \geq \alpha_{\rm crit} \approx \left(\frac{3}{4f_4^2|j_2|^2(1-\mu)e'^{|j_1+j_2|-2}} \left| \frac{C_{s1}}{C_r} \right| \right)^{1/(f_4|j_1|-5)} , \qquad (10)$$

where j_1 is also a function of α. Numerically, we observe that, regardless of the mass ratio and the resonance involved, $|C_{s1}/C_r|$ rises monotonically with f_4 and clusters around 0.02 when $f_4 \approx 0.5$. For simplicity, we solve for $\alpha_{\rm crit}$ considering only $f_4 \approx 0.5$. The results are plotted in Fig. 5 for three mass ratios. When only $j_2 = -1$ MMRs are considered, the $\mu = 0.1$ and $\mu = 0.2$ results sit atop each other falling somewhat below the respective HW99 curves at small values of e' and above them at large values. Besides errors resulting from our crude approximation in taking $f_4 = 0.5$, two other factors may contribute to this discrepancy. The first is that we are searching for the very minimum value of α at each value of e' that allows resonance overlap. As is shown in Fig. 2, this may lie up to 20% below the HW99 numerical result. The second factor is that we ignore overlap between distinct MMRs, which may be important at sufficiently large e'. When $\mu = 0.5$, our curve consistently sits above the HW99 line, resembling the discrepancy shown in Fig. 3. This, as we argue above, likely reflects failure of the expansion formula when μ is large (more below).

Despite these short-comings, this simple analysis yields some useful insight. Comparing overlap conditions between those resonances with $j_2 = -1$ and those with $j_2 = -2$, reveals that the latter resonances always occur at a larger value of α for a given e' value. They are therefore not important for determining the instability boundary and we conclude that our neglect of $|j_2| > 4$ MMRs is valid. This point is further emphasized in the inset of Fig. 2. Based on this conclusion, we argue that instability boundaries obtained from finite-duration numerical integration are reliable, even though they may not detect long-term instabilities brought about by very high-order resonances (e.g., 50:3). A second point con-

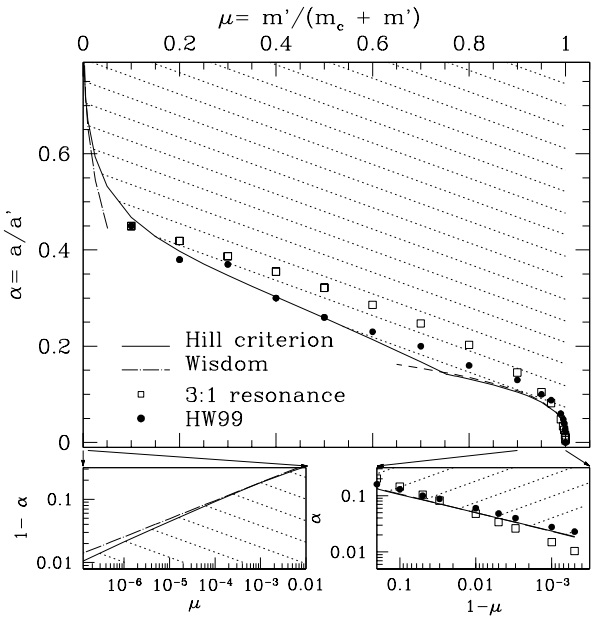

FIG. 6.—Instability boundary for circular binaries as a function of mass ratio μ. The solid curve depicts the result obtained based on the Hill criterion. Planets situated within shaded regions could potentially be ejected from the host star, though they will not be unless their orbits are chaotic. Overplotted are analytical results for the boundary of resonance overlap (and therefore chaos, but not necessarily ejection): as $\mu \to 0$, the overlap condition between $p+1$:p resonances yields $\alpha_{\rm crit} \geq 1-1.307\mu^{2/7}$ (Wisdom 1980a); for larger μ values, overlap between the $(3,-1,-1,-1)$ and $(3,-1,0,-2)$ sub-resonances occurs for α values above the open squares (this study). Locations of the open squares are calculated using expansion formula strictly valid only for $\mu \ll 1$. Also plotted (in filled circles) are the numerical results by HW99—planets situated above the filled circles are numerically shown to have unstable orbits. Left and right lower panels expand the view near $\mu = 0$ and $\mu = 1$, respectively. For $\mu \to 1$, the Hill criterion is well quantified as $(1/3)R_H = 0.23(1-\mu)^{1/3}$ (dashed curve).

cerns the fact that we have ignored terms of order μ^2 in the expansion of the disturbing function, and that our C_{s1} and C_r coefficients are only correct to order-of-magnitude. We argue, however, that the instability boundary depends only on the ratio of C_{s1}/C_r (eq. [10]). Moreover, if, for instance, the true ratio of C_{s1}/C_r is smaller by a factor of 10 than our adopted value of 0.02, the instability boundary for $\mu = 0.5$ is moved downward in α by as much as 10% (Fig. 5).

Our arguments here are based on very crude scaling relationships. They ought to be checked using more elaborate numerical experiments.

4. CIRCULAR, RESTRICTED THREE-BODY PROBLEM

We focus on $e' = 0$ binaries to study the following two issues: the applicability of the Hill criterion for predicting planet instability, and the relevance of 'bounded chaos' that prevents us from using resonance overlap as a synonym for planet instability.

With the exception of those of first and second-order, the widths of all other MMRs approach zero in circular binaries (see Appendix A). The resonance overlap condition in this limit is particularly easy to analyze. In the case where $\mu \to 0$ (the sun-asteroid-planet problem), Wisdom (1980a) derived the overlap condition between first-order $(p+1$:$p)$ resonances as described by $|1-\alpha| = |a'-a|/a' \leq 1.307\mu^{2/7}$ (also see Duncan et al. 1989; Malhotra 1998). For larger μ values, we argue that overlap between the $(3,-1,-1,-1)$ and $(3,-1,0,-2)$ sub-resonances defines the lowest α value for which chaos can set in. Note that we calculate the resonance location and width using expansion formulas that are strictly valid only for $\mu \ll 1$. We suspect this approximation may lead to some uncertainty in the results in Fig. 6. Moreover, we have not considered the 'evection resonance', which becomes important as $\mu \to 1$ (Touma & Wisdom 1998; Nesvorný et al. 2003).

The stability of planets in a circular binary can also be studied using the concept of Hill stability (e.g. see Murray & Dermott 1999). In such systems, there exists an integral of motion, the Jacobi constant, which defines permitted regions of planetary movement. For a planet that begins with a circular orbit around one star (as in HW99), there is a critical value of α below which the zero-velocity curve with the same Jacobi constant is 'closed' and the planet cannot escape. For values of α greater than this critical value, the planet is allowed to escape by the Hill criterion but will *not* unless its orbit is chaotic due to overlapping resonances. In other words, the Hill criterion is a necessary but not a sufficient condition for planet *instability*.

To calculate $\alpha_{\rm crit}$, one needs to carefully consider the phrase 'begins with a circular orbit.' For $\mu \ll 1$ systems (analogous to the sun-asteroid-planet problem), it is more appropriate to actualize this condition by taking the sidereal velocity (velocity in the binary center-of-mass frame) to be Gm_c/a; while for $\mu \to 1$ systems (analogous to the planet-satellite-sun problem), the more reasonable approach is to set the synodic velocity (in the host star's rotating frame) to be Gm_c/a. For intermediate μ values, we adopt the approach that yields the higher value of $\alpha_{\rm crit}$. The resultant values of $\alpha_{\rm crit}$ are plotted in Fig. 6 as a function of μ. In particular, in the limit where $\mu \to 1$, we find that $\alpha_{\rm crit} = (1/3)R'_H = [(1-\mu)/81]^{1/3}$ where R'_H is the Hill radius of the binary companion (Szebehely 1978), and in the limit where $\mu \ll 1$, we find that $\alpha_{\rm crit} = 1-2.1\mu^{1/3}$.

While the Hill criterion gives the energetic condition for planet instability, resonance overlap provides the dynamical cause. How do results from the Hill criterion compare with those from the resonance overlap criterion? Intriguingly, they seem to closely trace each other over small μ, intermediate μ and large μ values (Fig. 6). The only exception is when $\mu \to 0$ (visible when $\mu \leq 10^{-4}$) for which the resonance overlap occurs over a larger range than does the Hill criterion. Gladman (1993) has studied this limit and concluded that 'bounded chaos,' producing unpredictable but limited variations in the orbital elements, reigns in the intervening region. This instance, however, is the only clear sign of bounded chaos in the circular, restricted problem.

Numerical results by HW99 (filled circles in Fig. 6) and our own simulations also confirm this seemingly coincidental agreement between the resonance overlap condition and the Hill criterion. It appears then, that in practice, the Hill criterion is not only a necessary, but also a sufficient condition for planet instability.

5. CONCLUSIONS

A planet in a binary system experiences both secular and resonant perturbations from the binary companion. It may be dislodged from its host star if it is simultaneously affected by two resonances. We find that overlap between sub-resonances of the same MMR accounts for the instability observed by HW99 and our own numerical integration. There is little evidence for 'bounded chaos' and the word 'resonance overlap' can be interchanged with the word 'orbital instability'. Our instability boundaries largely agree with those obtained by

HW99, albeit with many fine features. The jutting peninsulas and deep inlets in the instability boundary correspond to the instability (or stability) islands first observed by HW99. The presence of these islands suggests that the longest-period stable orbit at each e' value could be reduced by as much as 20% from the HW99 value. Moreover, our analysis suggests that overlap between very high-order resonances (e.g., 50:3) do not substantially modify the instability boundary: these weak resonances, while producing slow chaotic diffusion, which may be missed by finite-duration numerical integrations, do not contribute markedly to planet instability.

In detail, the centroids of different sub-resonances are displaced from each other by the strong secular forcing of the companion enlarging the phase space of resonance overlap. Chaotic diffusion caused by sub-resonance overlap is observed to be fast, unlike cases in the solar system. The longest ejection timescale in our study, corresponding to sub-resonance overlap within the 30:1 MMR, is $\sim 10^6$ binary orbits, or, 1 Gyrs for a 100 AU solar-mass binary. For comparison, the 5:1 MMR overlap gives rise to an ejection time ~ 2000 binary orbits.

Compared with numerical integrations, our perturbation analysis has the following short-comings: the perturbation strength is calculated accurate only to first-order in the mass-ratio between the companion and the host star, and the perturbation formula diverges for $e' > 0.66$.

As a final note, we raise the issue of stability in circular binary systems ($e' = 0$). While the Hill criterion (critical Jacobi constant) gives the energetic condition for planet instability, resonance overlap provides the dynamical cause. We observe that over almost the entire range of mass-ratio, the Hill criterion and resonance overlap yield similar critical α values, making the Hill criterion not only a necessary, but also a sufficient condition for planet instability.

We thank M. Holman and S. Tremaine for helpful discussions, and an anonymous referee whose comments helped to improve the paper. This research was supported in part by the Natural Sciences and Engineering Research Council of Canada, as well as the National Science Foundation of the US under Grant No. PHY99-07949.

REFERENCES

Benest, D. 1993, Celestial Mechanics and Dynamical Astronomy, 56, 45
Beust, H. 2003, A&A, 400, 1129
Chirikov, B. V. 1979, Phys. Rep., 52, 265
David, E.-M., Quintana, E. V., Fatuzzo, M., & Adams, F. C. 2003, PASP, 115, 825
Dermott, S. F. & Murray, C. D. 1983, Nature, 301, 201
Duncan, M., Quinn, T., & Tremaine, S. 1989, Icarus, 82, 402
Duncan, M. J., Levison, H. F., & Lee, M. H. 1998, AJ, 116, 2067
Duquennoy, A. & Mayor, M. 1991, A&A, 248, 485
Dvorak, R. 1984, Celestial Mechanics, 34, 369
Eggenberger, A., Udry, S., & Mayor, M. 2004, A&A, 417, 353
Gladman, B. 1993, Icarus, 106, 247
Hénon, M. & Guyot, M. 1970, in Periodic Orbits Stability and Resonances, 349–+
Holman, M. J. & Murray, N. W. 1996, AJ, 112, 1278
Holman, M. J. & Wiegert, P. A. 1999, AJ, 117, 621
Lecar, M., Franklin, F., & Murison, M. 1992, AJ, 104, 1230
Lecar, M., Franklin, F. A., Holman, M. J., & Murray, N. J. 2001, ARA&A, 39, 581
Malhotra, R. 1998, in ASP Conf. Ser. 149: Solar System Formation and Evolution, 37–+
Marzari, F., Weidenschilling, S. J., Barbieri, M., & Granata, V. 2005, ApJ, 618, 502
Murray, C. D. 1992, Nature, 357, 542
Murray, C. D. & Dermott, S. F. 1999, Solar system dynamics (Cambridge University Press)
Murray, N. & Holman, M. 1997, AJ, 114, 1246
Musielak, Z. E., Cuntz, M., Marshall, E. A., & Stuit, T. D. 2005, A&A, 434, 355
Nesvorný, D., Alvarellos, J. L. A., Dones, L., & Levison, H. F. 2003, AJ, 126, 398
Pilat-Lohinger, E. & Dvorak, R. 2002, Celestial Mechanics and Dynamical Astronomy, 82, 143
Rabl, G. & Dvorak, R. 1988, A&A, 191, 385
Szebehely, V. 1978, Celestial Mechanics, 18, 383
Touma, J. & Wisdom, J. 1998, AJ, 115, 1653
Wisdom, J. 1980a, AJ, 85, 1122

APPENDIX

WIDTH OF A MEAN-MOTION RESONANCE UNDER SECULAR FORCING

MD99 have presented a derivation for the width of a MMR when the resonance angle evolves due to a single resonance. In our situation with a massive third body, secular effects on the resonance angle have to be taken into account. We show here how this modifies the resonance width and resonant centroid.

The relevant resonance angle as well as its time derivatives are,

$$\varphi_j = j_1\lambda' + j_2\lambda + j_3\varpi' + j_4\varpi, \tag{A1}$$

$$\dot{\varphi}_j = j_1 n' + j_2 n + j_4\dot{\varpi}, \tag{A2}$$

$$\ddot{\varphi}_j = j_2\dot{n} + j_4\ddot{\varpi}. \tag{A3}$$

The time-variations of n', e', ϖ', and ϵ' due to the influence of the planet are neglected as the planet can effectively be thought of as a test mass ($m/m_c \ll 1$). We also neglect variations in ϵ as previously mentioned.

We take the time-derivative of equation (6), substitute equations (5) and (6) into the right-hand side, and use the resulting equations to recast equation (A3) into the form

$$\ddot{\varphi}_j = \left[3j_2^2\tilde{C}_r n e^{|j_4|} + |j_4|^2\tilde{C}_r e^{|j_4|-2}(j_1 n' + j_2 n) - 2|j_4|^3 C_{s1}\tilde{C}_r e^{|j_4|-2}\right]\sin\varphi_j - |j_4|^3\tilde{C}_r{}^2 e^{2|j_4|-4}\sin 2\varphi_j, \tag{A4}$$

where $\tilde{C}_r = C_r e'^{|j_3|}$. This reduces to equation (8.63) of MD99 when $|j_4| = 1$ and $C_{s1} = 0$. In deriving this equation, we have made some simplifying assumptions. Firstly, we have ignored the time-dependence of C_{s1} and C_r, which are in reality both functions of α. Secondly, we have neglected the C_{s2} terms in equations (5) and (6) as we expect their time-averaged contributions to be negligible.

We look for a solution of the system that is pendulum-like, as in the case without secular forcing. Following MD99, we write $n = n_0 + k\cos[\varphi_j/2]$, where n_0 is the mean motion associated with the nominal value of the resonance and k is a constant that

describes the amplitude of the oscillation, or equivalently, the width of the resonance. The choice of the angular form, $\cos[\varphi_j/2]$, is determined by the libration amplitude of the resonant angle φ_j ($-\pi$ to π) as well as the presumed angle where maximum change in the mean motion occurs ($\varphi_j = 0$). The latter applies when $C_r < 0$ and shifts to $\varphi_j = \pi$ when $C_r > 0$; however, the final result does not depend on the presumed sign of C_r.

The derivation that follows is analogous to that presented in §8.7 of MD99. We do not repeat the details here but simply outline the results:

$$j_1 n' + j_2 n_0 = 2|j_4|C_{s1} + j_4^2|\tilde{C}_r|e^{|j_4|-2}, \tag{A5}$$

$$k = \frac{-2}{3}\frac{j_4^2}{j_2}|\tilde{C}_r|e^{|j_4|-2} \pm \sqrt{12|\tilde{C}_r|ne^{|j_4|}}\left(1 + \frac{j_4^4|\tilde{C}_r|e^{|j_4|-4}}{27 j_2^2 n}\right)^{1/2}. \tag{A6}$$

The secular term is important for shifting the centroid of the resonance, but does not contribute to the width of the resonance. In fact, the width formula is identical to equation (8.75) of MD99 where secular forcing is ignored.

The simple pendulum approach applies only when the resonant width is small, i.e., $\delta n = n_{\max} - n_{\min} \ll n$. Moreover, assuming that e is driven by the secular interaction to a value that is proportional to e' (eq. [8]), most MMRs have widths which approach 0 as $e' \to 0$. The first-order (e.g., 2:1) and second-order (e.g., 3:1) resonances that satisfy $j_4 \neq 0$ are exceptions; the width diverges for the former and approaches a constant for the latter.